

# Data encoding efficiency in pixel detector readout with charge information

Maurice Garcia-Sciveres<sup>b</sup>, Xinkang Wang<sup>a</sup>

<sup>a</sup>*University of Chicago, Chicago, IL, USA.*

<sup>b</sup>*Lawrence Berkeley National Laboratory, Berkeley, CA, USA.*

---

## Abstract

The minimum number of bits needed for lossless readout of a pixel detector is calculated, in the regime of interest for particle physics where only a small fraction of pixels have a non-zero value per frame. This permits a systematic comparison of the readout efficiency of different encoding implementations. The calculation is compared to the bits used for by the FE-I4 pixel readout chip of the ATLAS experiment.

*Keywords:* Particle tracking detectors (Solid-state detectors), Data acquisition concepts, Electronic detector readout concepts (solid-state), Data reduction methods, Information theory

---

## 1. Introduction

In reference [1] we presented a prescription for calculating the efficiency of readout encoding methods for binary strip detector readout, which is arguably the simplest case of interest for particle physics instrumentation. Here we extend the analysis to pixel detectors and also to include charge information rather than binary readout. Both the two-dimensional nature of pixel hit patterns and the addition of charge information introduce significant complexity. We preserve the same meaning of readout efficiency as the number of bits used in practice to extract all the required information from the detector, relative to the minimum possible number of bits needed given by the information content. Calculating this minimum is the main content of this note. This does not mean the bits used for a single event or readout cycle, but the average bits per event for a large ensemble of events. In practice we define efficiency as the minimum possible number over the actual number of

bits, so that it has a value between 0 and 1. We consider only lossless data compression, as opposed to data reduction in which information is discarded and cannot be recovered.

We consider typical pixel detector occupancy below 0.5%, where occupancy always means average occupancy over a fairly long time (eg. 1 second). The average occupancy is what determines the output data bandwidth requirement, rather than the instantaneous occupancy of a single event. The actual readout bandwidth required for a given occupancy depends on how much the data can be compressed, and also on the required latency (how long one is willing to wait for the information). We only consider the compression aspect here; for a case study that includes latency considerations see ref. [2].

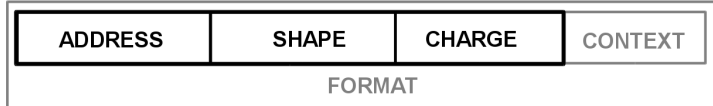


Figure 1: Schematic breakdown of the detector output data into component parts. The three bold face components are analyzed in this note.

Following ref. [1] we decompose the detector output data into the parts shown in Fig. 1, where we have added cluster shape and charge elements that were not present for binary strip detector readout. A cluster is any combination of hit pixels which are *touching*, including corner-to-corner touching. Any two hit pixels that touch belong to the same cluster. We will only study the bold face parts in this note, since the treatment of context and format elements given in ref. [1] remains valid. We have chosen this decomposition for convenience, but other decompositions are possible. The end result- the minimum number of bits possible to encode all the information, or information entropy- is a physical property and should not depend on the path chosen to calculate it. The decomposition of Fig. 1 has a first order physical interpretation as follows. The *addresses* correspond to the positions of particles crossing a silicon sensor- each particle forming one cluster that is identified by one address (the cluster address can be defined in several ways, for example as the bottom left corner pixel of the smallest box containing the cluster. How it is defined is not important to our discussion). The uniform distribution of particle tracks crossing a sensor makes the cluster address entropy straightforward to calculate. Each cluster has a *shape* and *size*, which are given by cluster distribution functions which depend on position, orientation,

and other features that may or may not vary across a particular detector. There are nevertheless a finite number of possible shapes and sizes. Finally, there is a *charge* distribution in each cluster. In the classical limit charge is an analog quantity and therefore a potential problem for an entropy calculation, which requires a discrete distribution. However, the practical measurement of charge is limited by noise, and we must therefore consider the entropy of encoding useful charge information, not meaningless noise fluctuations. For this we will further decompose charge into total charge,  $QT$ , and single pixel charge fractions,  $QF$ . To higher order, multiple particles can merge into one cluster, secondary interactions from a single particle can result in multiple clusters, and dead pixels or charge deposits that fluctuate below threshold can lead to split clusters. So the association of clusters to randomly incident single particles is not perfect, but as we will see at low occupancy such high order corrections have a negligible impact on the entropy.

Sections 2, 3, and 4 evaluate and discuss the address, shape, and charge entropy, respectively. The total information entropy due to the hits is the sum of these parts,

$$H_{\text{hits}} = H_A + H_s + (H_{QT} + H_{QF}) \quad (1)$$

which excludes the context and format contributions as already explained.

## 2. Address Entropy

In the limiting case of individual pixels rather than clusters, the address entropy is given simply by the logarithm of number of ways to pick  $k$  out of  $n$  pixels, where  $k/n$  is the occupancy and  $n$  is the number of pixels in the chip. This is given by the expression  $\log_2 \binom{n}{k}$ . When clusters are considered, two clusters cannot be touching, or they would count as a single cluster. One must therefore exclude a 1-pixel-wide empty boundary around each cluster. Let  $z$  be the total number of pixels associated with a cluster *including* this empty boundary. The address entropy then has a lower bound

$$H_z = \log_2 [\prod_{i=0}^{k-1} (n - zi)/(i + 1)] \quad (2)$$

which of course reduces to  $\log_2 \binom{n}{k}$  for  $z = 1$  (1-pixel clusters with no empty boundary).  $H_z$  is a lower bound because at the edges of a chip, or when two clusters are very close, a dedicated empty boundary for each one is not needed. Fig. 2 shows the ratio  $\log_2 \binom{n}{k}/H_z$  for  $z = 9$  (1-pixel clusters plus an

empty boundary) and  $z = 25$  (3 by 3-pixel clusters plus an empty boundary). It can be seen that, for the occupancy range of interest,  $\log_2 \binom{n}{k}$  and  $H_z$  are very close, and therefore  $H_A = \log_2 \binom{n}{k}$  is a good approximation to the true entropy. We will use  $H_A$  as the address entropy in our calculations.

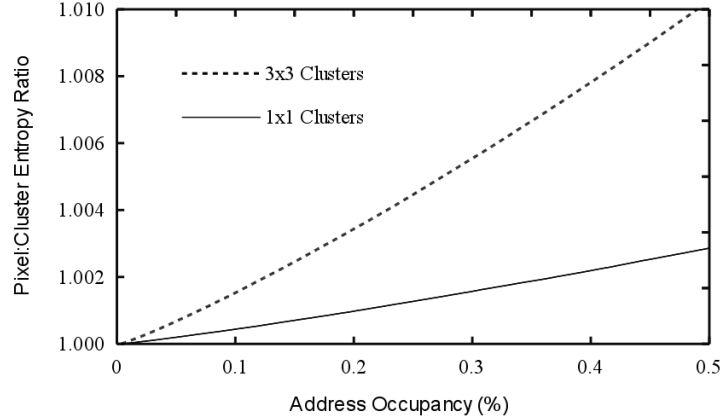


Figure 2: Ratio of single pixel address entropy to entropy of different size isolated clusters, as explained in the text.

It is instructive to examine the address entropy per address as a function of occupancy. For a single address, the entropy is simply the number of bits needed to count the full address space, so for a readout chip with  $2^{16}$  pixels the address entropy of a single address (occupancy of  $2^{-16}$ ) is 16 bits. But as the occupancy rises, fewer and fewer bits are needed per address. Within the occupancy range of interest, the number of bits per address quickly converges to a common value independent of chip size. Fig. 3 shows the address entropy per address as a function of occupancy for chips sizes  $2^{14}$ ,  $2^{16}$ , and  $2^{18}$  pixels (note that the occupancy range in this figure goes only up to 0.1% so that the difference between the curves can be appreciated). This is an important result counter to conventional wisdom. It shows that making a chip larger and therefore growing the address space (keeping pixel size constant) does *not* imply a greater data volume due to the need for more address bits. If addresses are compressed (rather than using the same number of bits per address regardless of occupancy), then approximately the same number of bits is needed to transmit the cluster address information regardless of chip size. Making pixels smaller, on the other hand, does increase the entropy per address as expected (i.e. cutting the pixel size in half adds one bit). This

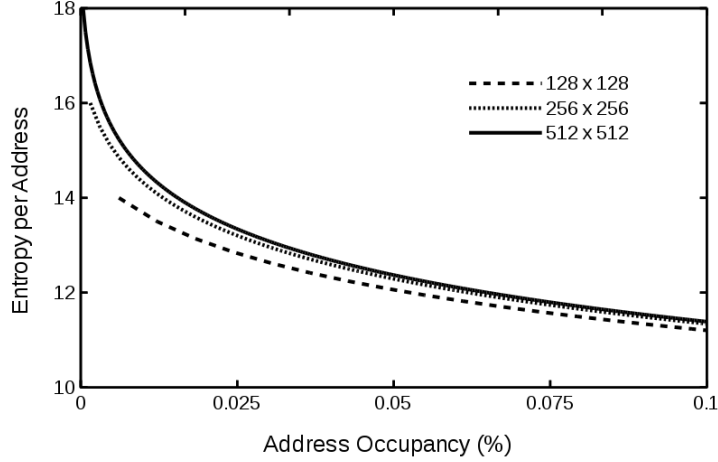


Figure 3: Address entropy per address as a function of address occupancy, for different size chips as indicated.

is more difficult to appreciate from Fig. 3, where reducing pixel size has the effect of reducing occupancy (so moving to the left on the curves) as well as increasing the number of pixels for constant size chip.

### 3. Shape Entropy

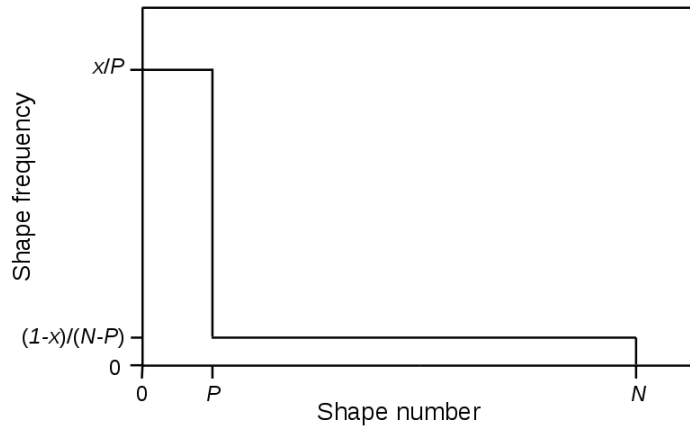


Figure 4: Representation of distribution of cluster shapes in an arbitrary readout unit

We consider shape to also include the size (number of pixels) of a cluster. A single pixel has zero shape entropy, but two adjacent pixels can have 4

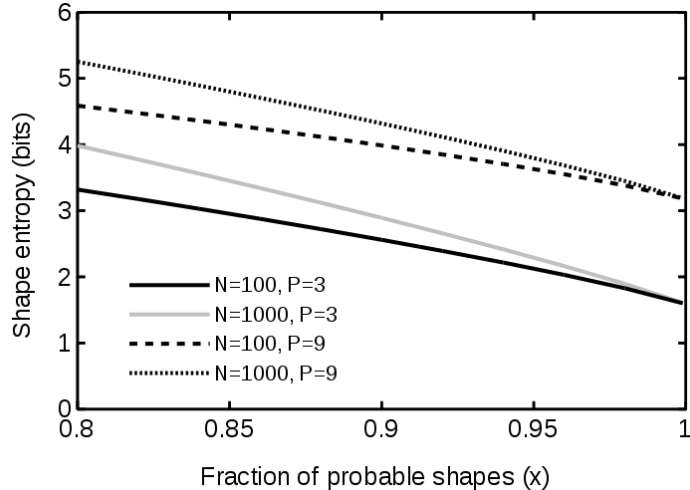


Figure 5: Shape entropy for different choices of  $N$ , the total number of cluster shapes, and  $P$ , the number of most frequent shapes making up the total fraction shown on the  $x$  axis.

possible shapes (up-down, left-right, and two diagonals). Three adjacent pixels can have 20 possible shapes, four pixels 110 shapes, and so on (see [3]). From this it seems that shape entropy can be rather large, and difficult to estimate in general. But in real-life particle detectors this will not be the case, and we can estimate a shape entropy without knowing a detailed cluster zoology. The reason is that each readout element of a pixel detector (a single chip or a multi-chip module) will be traversed by particles from a preferential direction, and these will produce similar-looking clusters. Thus, we can consider that some large fraction,  $x$ , of the clusters in a given readout unit consist of a small number of shapes,  $P$ , while the remaining  $1 - x$  can have a large variety of shapes,  $N - P$ , due to scattered particles and radiation. This is shown graphically in Fig. 4. The shape entropy is thus,

$$H_s = -x \log_2(x/P) - (1 - x) \log_2\left(\frac{1 - x}{N - P}\right) \quad (3)$$

$H_s$  is plotted for different  $N$  and  $P$  in Fig. 5. Not surprisingly, the shape entropy is dominated by the number of cluster shapes that occur very frequently, and the presence of hundreds of additional, but improbable shapes has little impact. For estimation purposes we will take 4 bits per cluster as a reasonable indicative value for shape entropy. However, the cluster shapes occurring frequently in one particular module of a pixel detector will be dif-

ferent from those in another module with different position relative to the collisions. Therefore, in order to realize in practice low entropy encoding of cluster shapes, each module would need to use a different encoding (a different Huffman table, for example), which would have to be programmed or learned by the module from its own data.

#### 4. Charge Entropy

We first consider cluster charge. The ideal cluster charge obeys a Landau distribution for a minimum ionizing particle passing through a silicon detector. In practice one must consider a spectrum of different particle momenta and incidence angles, which leads to a sum of Landaus, as well a Gaussian broadening due to noise. These effects are not important for this analysis. The results shown here were obtained using a cluster charge probability distribution function  $QT$  equal to the sum of 5 Landau distributions with means at  $\mu = 4, 5, 6, 7$ , and  $8$  arbitrary units, where the Landau function is  $QT(q) = \frac{1}{\sqrt{2\pi}} e^{-[q-\mu+e^{-(q-\mu)}]/2}$ . Using a single Landau instead made very little difference. The mean of  $QT$  is just the average of the means or  $6.5$ .

To compute an entropy we first “digitize” the charge PDF by histogramming it in  $2^D$  equal width bins in the range  $0$  to  $20$  ( $40$ ) arbitrary units. The last (overflow) bin is increased to that the total histogram probability is unity. Note that  $20$  ( $40$ ) corresponds to just over  $3$  ( $6$ ) times the mean of PDF. For each value of  $D$  we compute the entropy as  $H = -\sum_i p_i \log_2(p_i)$ , where the sum is over all histogram bins and  $p_i$  is the probability in each bin. We also compute the *digitization error* by performing a toy experiment in which we measure cluster charge in 4 hypothetical layers and take the average. This is representative of measuring the specific ionization of particle tracks in a silicon detector. The true value for each layer is randomly drawn from  $QT$ , while the measurement is taken to be the central value of the histogram bin that the true value falls into. The digitization error is the standard deviation of the difference between the average of the 4 measurements and the true average. The digitization error vs. cluster charge entropy,  $H_{QT}$ , is shown in Fig. 6.

As previously mentioned, we want to calculate the entropy for a meaningful charge measurement, and the most precise possible meaningful measurement is limited by noise. A horizontal line in Fig. 6 is included to represent the noise level. Obviously the noise level will vary from system to system, so this value is an example. We drew the line at  $0.0125$  which means  $S/N=80$

for the average of 4 measurements. This shows that for this particular noise level the cluster charge entropy is  $H_{QT} = 4.2$  bits per cluster. Fig. 6 also includes two additional curves to show the bits per cluster for an uncompressed linear ADC scales for the two dynamic ranges considered: 20 units and 40 units (the dynamic range has no effect on the calculated entropy). We also explicitly compressed the ADC values using Huffman codes, and the average number of bits after compression matched calculated entropy for both dynamic ranges.

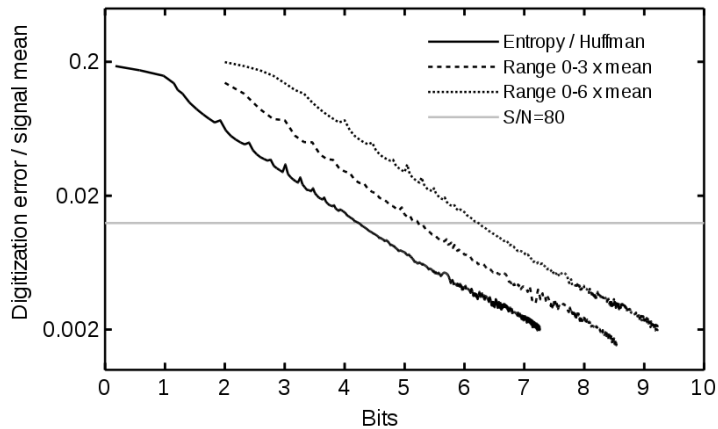


Figure 6: Digitization error for average of 4 measurements (4 layers) vs. number of bits used in digitization. The 0-3 x mean and 0-6 x mean ranges refer to the digitization range for which the binary ADC value is transmitted without compression. Compressing the ADC value using Huffman codes achieves the entropy value regardless of the ADC range.

In addition to cluster charge, we must also consider the charge of individual pixels in a cluster. The single pixel charge distribution does not have a universal Landau form. As we already have analyzed the cluster charge, the remaining information is not the absolute charge, but the fraction of the total cluster charge in each pixel. The analysis is particularly simple for a 2-pixel cluster. As both pixels must have the same charge fraction distribution  $F$ , it follows that  $F$  must be symmetric  $F(r) = F(1 - r)$ , where the fraction  $r$  ranges between 0 and 1. Furthermore, in the ideal case that the charge splitting is due to the ionizing particle that created the cluster crossing the boundary between the pixels (as opposed to a systematic effect like electronic crosstalk), then there is no favored splitting and the ratio distribution is simply  $F = 1$ . Thus,  $F$  is digitized in  $2^D$  equal size bins with equal probability in each bin and the entropy is simply  $D/2$  per pixel ( $D$  is divided

by 2 because only the charge fraction in one pixel need be specified). The smallest useful bin size should be simply given by the single pixel noise over the single pixel average signal. Thus, for 2-pixel cluster S/N=40, the signal to noise on the single pixel fraction will be approximately 20. Hence,  $H_{QF} = \log_2(20)/2 = 2.15$  per pixel. We will take this as a general estimate in average. Clearly for individual clusters  $H_{QF}$  will vary:  $H_{QF} = 0$  for 1-pixel clusters, and  $H_{QF} > 2 \times 2.15$  for more than 2-pixel clusters.

## 5. Combined Result

We can now combine the above estimates to obtain a value for  $H_{\text{hits}}$  of Eq. 1, which we write as an entropy per cluster. From Fig. 3 we see that  $H_A/N_{\text{cluster}} \approx 12$ . From Fig. 5 we can estimate that  $H_s/N_{\text{cluster}} \approx 4$ . From Fig. 6  $H_{QT}/N_{\text{cluster}} = 4.2$ . Also  $H_{QF}/N_{\text{pixel}} = 2.15$ . All these estimates are independent of fine details about the detector in question other than signal/noise. One parameter needed is the average number of hit pixels per cluster, due to  $H_{QF}$ . Taking a typical value of  $N_{\text{pixel}}/N_{\text{cluster}} \approx 2$  yields,

$$H_{\text{hits}}/N_{\text{cluster}} \approx 24.5 \quad (4)$$

As a concrete example we can compare this to the number of bits per cluster used by the FE-I4 chip of the ATLAS experiment [4], excluding format and context information, for an average cluster size of 2. For a  $2^{16}$  ( $2^{18}$ ) pixel chip, the number of bits for a 1-pixel cluster used by the FE-I4 encoding is 24 (26). For a 2-pixel cluster it can be 24 (26) or 48 (52), depending on the shape, and for a 3-pixel cluster 48 (52) or 72 (78). The FE-I4 encoding includes 4 bits of uncompressed ADC value per pixel, which is not sufficient a S/N=40 cluster charge measurement even with limited dynamic range (Fig. 6). The average number of bits depends on the cluster distributions. Using ATLAS experiment inner layer distributions [5] yields an average of 35 (37) bits per cluster.

## 6. Conclusion and Outlook

We have shown that it is possible to estimate the entropy of pixel detector hit data in the occupancy range of interest to particle physics, without knowing all the details about a specific detector. Approximate knowledge about the occupancy, signal to noise, and cluster size distributions is sufficient. This is useful to understand how much room for improvement there is

when developing a new detector readout. In particular, new pixel detectors for the High Luminosity LHC [6, 7] will have very high data volume, requiring efficient encoding of the information to be transmitted. A comparison to the readout encoding used by the ATLAS FE-I4 shows that, even with reduced signal to noise capability, the FE-I4 encoding has of order 40% bandwidth to be gained from data compression. With smaller pixels and therefore broader cluster size distributions, the gains from applying on-chip data compression will likely be even greater in future detectors. This work was supported in part by the Office of High Energy Physics of the U.S. Department of Energy under contract DE-AC02-05CH11231.

## References

- [1] M. Garcia-Sciveres and X. Wang, *Data encoding efficiency in binary strip detector readout*, *jinst* 9 P04021 (2014).
- [2] M. Garcia-Sciveres and X. Wang, *Data compression considerations for detectors with local intelligence*, *jinst* 9 C10011 (2014).
- [3] D. Redelmeier, “Counting polyominoes: Yet another attack,” *Discrete Mathematics* 36, Issue 2, pp191203 (1981).
- [4] M. Garcia-Sciveres *et al.*, “The FE-I4 pixel readout integrated circuit,” *Nucl. Instr. Meth.* A636 S155S159 (2011).
- [5] A. La Rossa (ATLAS Collaboration), “ATLAS Pixel Detector: Operational Experience and Run-1 to Run-2 Transition,”, *PoS Vertex2014*, C14-09-15.2 (2015).
- [6] R. Bates *et al.*, “ATLAS pixel upgrade for the HL-LHC,” to appear in *Proc. Vertex2015*, Santa Fe, USA (2015).
- [7] J. Butler *et al.*, “Technical Proposal for the Phase-II Upgrade of the CMS Detector,” *CERN-LHCC-2015-010* (2015).